Spectroscopic study of a bis(imidazole)(octaethylporphyrinato)iron(III) complex

Iwona Rutkowska,
Kazimierz Dziliński,
Tomasz Kaczmarzyk,
Jan Stanek

Abstract. Low-spin ferric octaethylporphyrinatoiron complex with two imidazole axial ligands $[Fe(III)(OEP)(Im)_2]^+$ has been investigated by electron paramagnetic resonance (EPR) and Mössbauer spectroscopies. It was found that the ground spin state corresponds to the electron configuration $(dxy)^2 (dxz, dyz)^3$ and planes of the imidazole axial ligands have a parallel mutual orientation. Ethyl groups bonded to pyrrole rings, as peripheral substituents, effect on the ground electron spin state of the complex studied and the relative orientation of the the imidazole axial ligands in a similar way like the phenyl substituents bonded to *meso*-carbon atoms of the porphyrin macrocycle. The temperature dependence of the Mössbauer spectra is discussed in terms of magnetic relaxation processes.

Key words: electron paramagnetic resonance (EPR) spectroscopy • Mössbauer spectroscopy • low-spin iron porphyrin • imidazole axial ligands

I. Rutkowska, K. Dziliński✉, T. Kaczmarzyk
Institute of Physics,
Częstochowa University of Technology,
19 Armii Krajowej Ave., 42-200 Częstochowa, Poland,
Tel.: +48 34 325 0795,
E-mail: dzil@wip.pczt.pl

J. Stanek
Marian Smoluchowski Institute of Physics,
Jagiellonian University,
4 Reymonta Str., 30-059 Kraków, Poland

Introduction

Iron porphyrins participate in the biological cycles as the heme prosthetic groups in hemoproteins such as hemoglobin and myoglobin as well as some cytochromes, peroxidases and catalases [12]. Iron ions, placed at the centre of the prosthetic groups, play a key role in biological processes which involve hemoproteins. Sufficient background information on the relationship between the porphyrin ligand structure and the electronic configuration of the iron ions is provided to form a basis for discussion on the complex bioprocesses. Apart from the biological aspects, the molecular structure and physical properties of iron porphyrins promote these complexes for application in such contemporary technologies as non-linear optics, molecular semiconductors, liquid crystals and so on [11].

Iron porphyrin complexes can change their electronic and coordination structures during the running of complex biological processes, so it is important to reveal the detailed information on various iron porphyrin complexes with different electronic and coordination structures. There is a wide variety of oxidation and spin states observed in iron porphyrins [17]. Through extensive studies, using various experimental techniques and theoretical methods, it has been established that the electronic configurations of iron ions in porphyrin

complexes are controlled in the nature by a number of axial ligands, peripheral substituents attached to the porphyrin macrocycle, deformation of the porphyrin ring and solvent effects [6, 13, 22]. In the case of the six-coordinate iron(III) complexes, carrying axial ligands with a relatively strong field strength such as imidazole, they exhibit usually a low-spin ($S = 1/2$) state. There are two types of electronic configurations in low-spin iron(III) porphyrin complexes – a commonly observed $(dxy)^2 (dxz, dyz)^3$ and a less common $(dxz, dyz)^4 (dxy)^1$ [13, 22]. On the basis of theoretical and spectroscopic studies, one can notice that complexes carrying axial ligands with strong σ-donating and weak π-accepting ability, such as imidazole, adopt most often the $(dxy)^2 (dxz, dyz)^3$ ground spin state, like in the case of bis(imidazole) iron(III) tetraphenylporphyrins [Fe(III)(TPP)(Im)₂]⁺ [24] but magnetic and EPR studies of the six-coordinate bis(2-metylimidazole)(octaethylporphinato)iron(III) complex [Fe(III)(OEP)(2-MeIm)₂]⁺ indicate a thermal spin equilibrium ($S = 1/2 \leftrightarrow S = 5/2$) with different contributions of the low-spin ($S = 1/2$) and high-spin ($S = 5/2$) components in solution and in solid state [7]. The authors of the paper [7] suggest that the mixed spin state and its dependence on the liquid or crystalline state is a result of the axial ligand orientation with respect to the pyrrole rings in the porphyrin macrocycle. It is interesting to know how peripheral substituents, such as ethyl groups, in comparison with the phenyl ones, effect on the electron configuration of Fe(III) ions in bis(imidazole) porphyrin complexes and orientation of the axial ligands.

In this paper, spectroscopic studies of bis(imidazole)(octaethylporphinato)iron(III) complex, [Fe(III)(OEP)(Im)₂]ClO₄, using EPR and Mössbauer methods are presented. To our knowledge, this complex has not been investigated so far and spectroscopic results presented here will be useful for further examinations of important biological objects, such as cytochromes *b*, by model systems. Molecular structure of the complex studied is shown in Fig. 1.
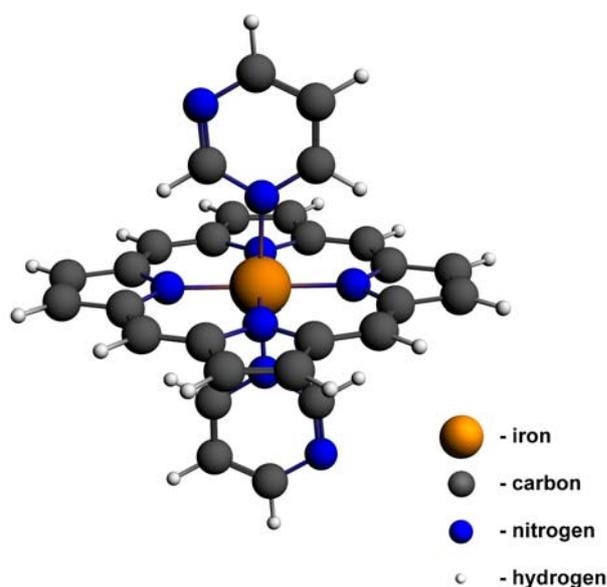
Fig. 1. Molecular structure of [Fe(III)(OEP)(Im)₂]⁺ with parallel orientation of imidazole axial ligands.

Experimental

Fe(OEP)ClO₄ was synthesized according to the procedures described by Dolphin *et al*. [4, 16]. The bis(imidazole) derivative of [Fe(OEP)(Im)₂]ClO₄ was obtained by the same general procedures as for the bis(2-methylimidazole) [Fe(OEP)(2-MeIm)₂]ClO₄ complex [7]. It should be noted that according to the crystal structure analysis [7] the [Fe(OEP)(2-MeIm)₂]ClO₄ complex consists of two ions – [Fe(III)(OEP)(2-MeIm)₂]⁺ cation and perchlorate anion [ClO₄]⁻, which are not bonded directly one with other. The average distance between them in the crystalline state is equal to about 3 Å [7]. The subject of our investigation is a ferric [Fe(III)(OEP)(Im)₂]⁺ complex. Tetrahydrofuran (THF) solvent was carefully degassed by freeze-thow cycles with the use of metallic potassium. EPR measurements were performed at liquid-nitrogen temperature using a conventional X-band spectrometer, equipped with an IBM PC data acquisition system. Mössbauer spectra were performed at $6 \div 295$ K and obtained with a ⁵⁷Co(Rh) source. A metallic iron foil absorber was used to calibrate the velocity scale, and isomer shifts are given vs. metallic Fe. Samples for Mössbauer measurements were in the form of pellets prepared from a powder obtained after evaporation of THF solvent. The samples contained about $4–10^{-4}$ g/cm² of ⁵⁷Fe. The EPR and Mössbauer parameters were found by fitting the experimental spectra to the theoretical ones using least-squares procedures.

Results and discussion

EPR spectra

In the case of low-spin iron(III) porphyrin complexes, there are three types of EPR spectra. Complexes that show the $(dxy)^2 (dxz, dyz)^3$ electronic configuration exhibit either rhombic or large g_{max} type spectra, depending on the mutual orientation of planar axial ligands such as imidazole. The complexes with parallel-aligned axial ligands show rhombic type spectra, while those with perpendicularly aligned axial ligands show large g_{max} type spectra [13]. In the case of the $(dxz, dyz)^4 (dxy)^1$ ground state EPR spectra usually show axial type, exhibiting single feature signals with g_{max} within the range $3.41 \div 3.78$ [13, 15, 20, 22]. EPR parameters can be used to estimate the relative energies of *d*-orbitals of iron ions that are the centres of biological activity of the hemoproteins. The EPR spectrum of the [Fe(III)(OEP)(Im)₂]⁺ complex is shown in Fig. 2.

This spectrum is typical of most bis-ligated d^5 porphyrin complexes [13, 24] and has a characteristic pure rhombic shape. Three *g*-values obtained from the spectrum, detected from THF solution and powder samples at 80 K, are presented in Table 1. The mentioned above parameters are typical of low-spin ferric porphyrins and cytochromes, and the [ClO₄]⁻ counterion does not affect values of EPR parameters [13, 24]. Some variations in *g*-values for the solution and powder samples can be caused by subtle distinctions in distortions changes of the porphyrin rings and axial ligands in both states. The relative energies of the d_{xy}, d_{xz} and d_{yz} orbitals can be arranged according to the scheme shown in Fig. 3.

Table 1. EPR parameters of bis(imidazole) Fe(III)-porphyrins

| Complex	Solvent	g_x	g_y	g_z	V/λ	Δ/λ	V/Δ	Ref.
[Fe(III)(OEP)(Im)$_2$]$^+$	THF	1.401	2.180	2.994	1.64	3.29	0.50	this paper
[Fe(III)(OEP)(Im)$_2$]$^+$	powder	1.441	2.198	2.946	1.74	3.30	0.53	this paper
[Fe(III)(TPP)(Im)$_2$]$^+$	CHCl$_3$	1.565	2.292	2.873	2.05	3.24	0.63	[24]
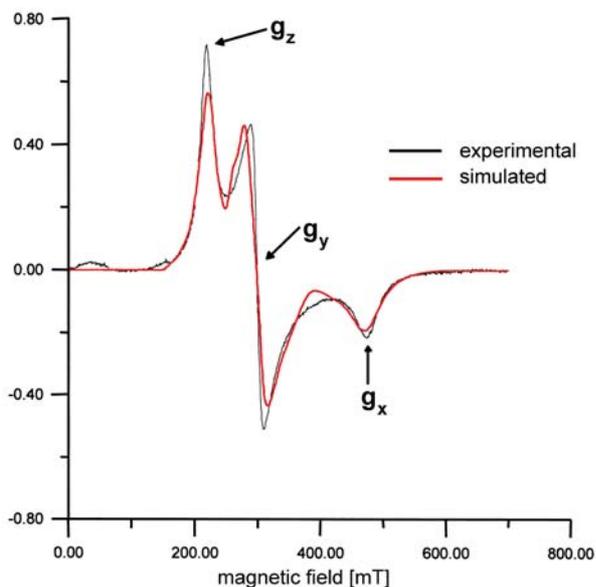
Fig. 2. EPR spectrum of [Fe(III)(OEP)(Im)$_2$]$^+$ in THF solution at 80 K.

Parameters of the rhombically distorted systems, such as tetragonal splitting Δ and rhombic splitting V, given in units of the spin-orbit coupling constant λ, can be estimated according to the expressions [17]

$$(1) \qquad V/\lambda = E_{yz} - E_{xz} = \frac{g_x}{g_z + g_y} + \frac{g_y}{g_z - g_x}$$

$$(2) \qquad \Delta/\lambda = E_{xz} - E_{xy} - \frac{1}{2}V/\lambda\frac{g_x}{g_z + g_y} + \frac{g_z}{g_y - g_x}$$

$$-\frac{1}{2}V/\lambda$$

It should be noted that the maximum g-value is taken to be g_z and this notation corresponds to an axis system when the orientation of the z-axis is perpendicular to the plane of the porphyrin ring. The x and y-axes lie along the bisector of pyrrole rings (Fig. 1). Equations (1) and (2) are valid as long as the remaining two empty orbitals $d_{x_2-y_2}$ and d_{z_2} lie sufficiently high in energy such their contribution can be neglected. The rombicity V/λ
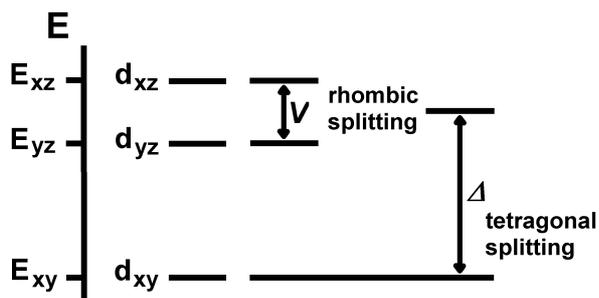
Fig. 3. Splitting of d-orbitals essential for the low-spin electron configuration of Fe(III) porphyrins.

and tetragonality Δ/λ values are shown in Table 1. For comparison, Table 1 contains also the EPR parameters for bis(imidazole) Fe(III)tetraphenylporphyrin [Fe(III)(TPP)(Im)$_2$]$^+$ which is associated with Cl$^-$ counterion.

It follows from the data listed in Table 1 for the THF solution and powder samples that the effect of solvent on the values of the EPR parameters and relative arrangement of d-orbitals is rather small. However, the porphyrin peripheral substituents such as the eight ethyl and four phenyl groups show somewhat more significant effect upon the d-orbital energies of the low-spin Fe(III) ions, in comparison with the solvent effect. Angular orientation of the imidazole ligands with respect to each other can also be established on the basis of the EPR data. Among two main orientations of the planes of two imidazole ligands attached to a Fe-porphyrin complex – mutually parallel or mutually perpendicular, the values of the EPR parameters shown in Table 1 indicate the parallel (or nearly parallel) relative orientation [13, 21, 25]. The smaller value of the rhombic distortion V/λ the larger deviation of the axial imidazole ligands from the mutual parallel orientation. Low-spin Fe(III) porphyrin complexes with an angle between two axial imidazole planes of less than 70° display rhombic EPR spectra [23]. The low-spin state of Fe(III) ions in the complex studied corresponds to the electron configuration which can be written as $(d_{xy})^2(d_{xz}, d_{yz})^3$ [13, 14]. So, the EPR data for the [Fe(III)(OEP)(Im)$_2$]$^+$ indicate a similar electron configuration of the Fe(III) ion and the mutual orientation of the imidazole axial ligands like in the case of the [Fe(III)(TPP)(Im)$_2$]$^+$. The ethyl peripheral substituents, attached to pyrrole rings, influence the ground electron spin state in a similar way like the phenyl substituents bonded to *meso*-carbon atoms.

Mössbauer spectra

Mössbauer spectroscopy is a very useful tool for characterizing subtle details of electronic structure of natural hemoproteins and their simpler models containing Mössbauer-sensitive elements – iron. Mössbauer spectra for powder samples of the [Fe(III)(OEP)(Im)$_2$]$^+$ complex are shown in Fig. 4.

Parameter values of these spectra are listed in Table 2. Besides the main parameters such as isomer shift (IS), quadrupole splitting (QS) and the linewidth (Γ) for Lorentzian shape, the surface ratio (A_{21}) and linewidth ratio (W_{21}) of the doublet components (higher energy absorption line of the doublet to the lower energy absorption component) are also shown. The A_{21} ratio was introduced to analyze mechanisms which can lead to the increase of the asymmetry as the temperature is lowering, and the W_{21} parameter can be used for numerical description of the observed asymmetry. It follows from the data collected in Table 2 that the values of the isomer shifts and quadrupole splittings are
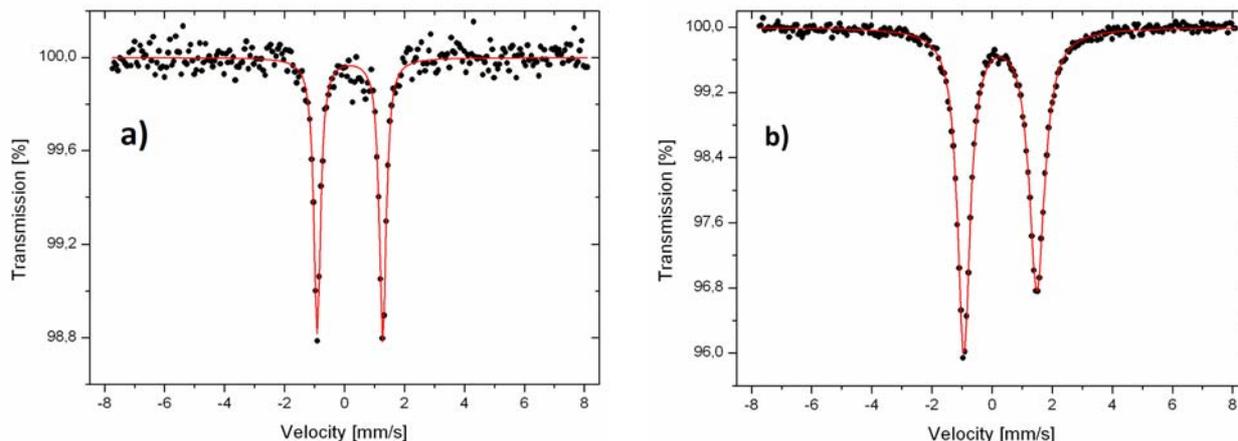
Fig. 4. Mössbauer spectra of [Fe(III)(OEP)(Im)$_2$]$^+$ complex at: (a) room temperature, (b) 6 K.

Table 2. Mössbauer parameters of the [Fe(III)(OEP)(Im)$_2$]$^+$ at different temperatures

Temperature (K)	IS (mm/s)	QS (mm/s)	Γ (mm/s)	A_{21}	W_{21}
295	0.18	2.19	0.27	1.043	1.007
240	0.20	2.27	0.28	1.021	1.062
160	0.24	2.36	0.30	1.037	1.247
77	0.26	2.41	0.48	1.000	1.223
6	0.28	2.43	0.51	0.990	1.231

within the range typical for the low-spin Fe(III) state [3, 20]. It was found earlier [20] that the quadrupole splittings are sensitive to the axial ligand orientation and some range of parallel and perpendicular relative orientations can be distinguished. Mössbauer study of crystalline low-spin ferriheme complexes has shown that, in general, the smaller dihedral angles between planes of the imidazole axial ligands the higher values of the quadrupole splitting. For instance, QS = 1.70 mm/s was found for bis(1-methylimidazole)(octamethylteraphenylporphynato)iron(III) [Fe(OMTPP)(1-MeIm)$_2$]$^+$ (dihedral angle close to 90°) and QS = 2.24 mm/s for bis(1-methylimidazole)(teramethylporphynato)iron(III) [Fe(TMP)(1-MeIm)$_2$]$^+$ (dihedral angle close to 0°) [20]. The QS value for the [Fe(TMP)(1-MeIm)$_2$]$^+$ complex is very close to QS from Table 2 for the [Fe(III)(OEP)(Im)$_2$]$^+$ complex under consideration in this paper.

Let us discuss briefly the questions due to temperature dependence of the isomer shifts and quadrupole splittings. One can notice that both parameters IS and QS are slightly continuously increasing with decreasing temperature in the range 295–6 K. Because of lack of phase transitions in these compounds, the temperature change of the observed isomer shifts should be attributed to the second order Doppler shift IS$_{SOD}$ [18]. Because the sign of the second order Doppler shift is negative, so the smaller absolute value of the IS$_{SOD}$ the greater positive value of the experimentally observed isomer shift. The temperature dependence of the IS$_{SOD}$ is assigned to decreasing of the mean square velocity $<\upsilon^2>$ of the Mössbauer atom induced by lattice vibrations with temperature decreasing and the value of the observed isomer shift IS becomes somewhat higher [10]. The temperature dependence of the quadrupole splitting QS may be explained by the thermal population of electronic states which are energetically close to each other [3], but other reasons should be considered

as well. For example, in the studied case, the decrease of temperature can lead to decreasing deviations from relative parallel orientations of the axial imidazole ligands and this reason can influence some increasing of the quadrupole splitting.

Characteristic feature of the asymmetry observed in the temperature study of the [Fe(III)(OEP)(Im)$_2$]$^+$ spectra is that higher-energy (higher-velocity) component of the doublet is more broadened than the lower-energy one (see Table 2 – W_{21} parameter is larger than one). The A_{21} values (Table 2) are very close to one, so the Goldanskii-Karyagin effect [8] seems to be negligible in consideration the asymmetry observed in the spectra of the [Fe(III)(OEP)(Im)$_2$]$^+$ complex. Thus, the observed at low temperature asymmetry should be related to the magnetic relaxation processes which the relaxation time approaching 141 ns, the characteristing time of the observation in the ^{57}Fe Mössbauer spectroscopy. The fact, that the high energy line in the quadrupole doublet of the Mössbauer spectrum exhibits bigger broadening is the evidence that the V_{zz} component of electric field gradient, acting on the ^{57}Fe nuclei, is positive [2]. This means that the Fe ion has a more negative charge in the porphyrin plane than in the perpendicular direction, confirming the $(d_{xy})^2(d_{xz}, d_{yz})^3$ ground state which follows from the EPR data, presented in this paper. If asymmetry of the doublets increases when temperature is lowering, it suggests that spin-lattice relaxation processes dominate over the weakly temperature dependent spin-spin relaxation ones [9]. In the case of the spin-lattice relaxation iron ions interact with the lattice by spin-orbit and orbital-phonon coupling which is related to fluctuations in the electrostatic crystal field potentials or to lattice vibrations [1]. Since the matrix elements of the orbital angular momentum do not vanish for the low-spin state of Fe(III)-porphyrins, the effect of the spin-lattice relaxation on the asymmetry of the spectra is expected

to be more essential in comparison with the spin-spin relaxation, although some spin-spin relaxation, through the energy transfer which occurs between interacting Fe(III) ions via dipole (or exchange) coupling, can be possible. It is interesting to note, that, as it has been shown recently [5, 19] the magnetic intermolecular interactions can determinate the relaxation time in Fe-porphyrins.

Conclusions

Summing up, we can conclude that the EPR and Mössbauer data, obtained for the $[Fe(III)(OEP)(Im)_2]^+$ complex, indicate the electron configuration of the low-spin Fe(III) ion in this complex denoted as $(d_{xy})^2(d_{xz}, d_{yz})^3$. Relative orientation of the imidazole axial ligands is nearly parallel. Ethyl groups bonded to the pyrrole rings as peripheral substituents effect on the ground electron spin state of this complex and relative orientation of the the imidazole axial ligands in a similar way like the phenyl substituents bonded to *meso*-carbon atoms of the porphyrin macrocycle. The temperature dependence of Mössbauer parameters and asymmetry of the spectra imply the dominant character of the spin-lattice relaxation over the spin-spin one.

References

1. Bizzari AR, Iakovleva OA, Parak F (1995) Spin-lattice relaxation in Mössbauer spectra of metmyoglobin: investigation of crystals, water and water-glycerol solutions. Chem Phys 191:185–194
2. Blume M, Tjon J (1968) Mössbauer spectra in fluctuating enviroment. Phys Rev A 152:345–357
3. Debrunner PG (1989) Mössbauer spectroscopy of iron porphyrins. In: Lever ABP, Gray HB (eds) Iron porphyrins. Part III. VCH Publishers, New York, pp 140–234
4. Dolphin DH, Sams JR, Tsin TB (1977) Intermediate-spin (S=3/2) porphyrinato-iron(III) complexes. Inorg Chem 16:711–713
5. Dziedzic-Kocurek K, Okła D, Stanek J (2013) Inter- and intramolecular dynamics of iron porphyrins. Nukleonika 58;1:83–86
6. Galstyan AS, Zaric SD, Knapp E-W (2005) Computational studies on imidazole heme conformations. J Biol Inorg Chem 10:343–354
7. Geiger DK, Lee YJ, Scheidt WR (1984) Control of spin state in (porphinato)iron(III) complexes. An axial ligand orientation effect on the spin state in bis(2-methylimidazole)(octaethylporphinato)iron(III) perchlorate. J Am Chem Soc 106:6339–6343
8. Goldanskii VI, Herber RH (eds) (1968) Chemical applications of Mössbauer spectroscopy. Academic Press, New York
9. Gutlich P, Link R, Trautwein A (eds) (1978) Mössbauer spectroscopy and transition metal chemistry. Springer, Berlin, pp 4–40
10. Kaczmarzyk T, Jackowski T, Dzilinski K, Sinyakov GN (2007) Asymmetry in Mössbauer spectra of Fe(III)-azaporphyrin complexes. Nukleonika 52;Suppl 1:S93–S98
11. Kadish KM, Smith KM, Guilard G (eds) (2000) The porphyrin handbook. Vol. 6. Applications: Past, present and future. Academic Press, San Diego
12. Kadish KM, Smith KM, Guilard G (eds) (2003) The porphyrin handbook. Vol. 11: Bioinorganic and bioorganic chemistry. Academic Press, Amsterdam
13. Kadish KM, Smith KM, Guilard R (2010) Electronic and magnetic structures of iron porphyrin complexes. In: Kadish KM, Smith KM, Guilard R (eds) Handbook of porphyrin science. Vol. 7. Word Scientific, New Jersey, London, pp 22–57
14. Liao M-S, Huang M-J, Watts JD (2010) Iron porphyrins with different imidazole ligands. A theoretical comparative study. J Phys Chem A 114:9554–9569
15. Mitiga CT, Iwazumi M (1981) Low-temperature EPR studies of highly anisotropic low-spin (protoporphyrinato) iron(III) complexes. J Am Chem Soc 103:4378–4381
16. Ogoshi H, Watanabe E, Yosida L et al. (1973) Synthesis and far-infrared spectra of ferric octaethylporphyne complexes. J Am Chem Soc 98:2845–2849
17. Palmer G (1983) Electron paramagnetic resonance of hemoproteins. In: Lever ABP, Gray HB (eds) Iron porphyrins. Part II. Addison-Wesley Publishing, London, pp 52–64
18. Shenoy GK, Wagner FE, Kalvius GM (1978) The measurement of the isomer shift. In: Shenoy GK, Wagner FE (eds) Mössbauer isomer shifts. North-Holland Publishing, Amsterdam, pp 49–110
19. Stanek J, Dziedzic-Kocurek K (2010) Magnetism of ferriprotoporphyrin IX monomers and dimers. J Magn Magn Mater 332:999–1003
20. Teschner T, Yatsunyk L, Schunemann V et al. (2006) Models of the membrane-bound cytochromes: Mössbauer spectra of crystalline low-spin ferriheme complexes having axial ligand plane dihedral angles ranging from 0° to 90°. J Am Chem Soc 128:1379–1389
21. Walker FA (1999) Magnetic spectroscopic (EPR, ESEEM, Mössbauer, MCD and NMR) studies of low-spin ferriheme centers and their corresponding heme proteins. Coord Chem Rev 185/186:471–534
22. Walker FA (2000) Proton NMR and EPR spectroscopy of paramagnetic metalloporphyrins. In: Kadish KM, Smith KM, Guilard R (eds) The porphyrin handbook. Vol. 5. Academic Press, San Diego, pp 81–183
23. Walker FA (2004) Models of the bis-histidine-ligated electron-transferring cytochromes. Comparative geometric and electronic structure of low-spin ferro- and ferrihemes. Chem Rev 104:589–615
24. Walker FA, Reis D, Balke VL (1984) Models of the cytochromes *b*. EPR Studies of low-spin iron(III) tetraphenylporphyrins. J Am Chem Soc 106:6888–6898
25. Yatsunyk LA, Carducci MD, Walker AF (2003) Low-spin ferriheme models of the cytochromes: correlation of molecular structure with EPR spectral type. J Am Chem Soc 125:15986–16005